(Ba,Ca)(Zr,Ti)O3 lead-free piezoelectric ceramics – the critical role of processing on properties

Bai, Yang; Matousek, A.; Tofel, P.; Bijalwan, Vijay; Nan, Bo; Hughes, Hana; Button, Timothy

DOI:
10.1016/j.jeurceramsoc.2015.05.010

Document Version
Peer reviewed version

Citation for published version (Harvard):
Bai, Y, Matousek, A, Tofel, P, Bijalwan, V, Nan, B, Hughes, H & Button, T 2015, '(Ba,Ca)(Zr,Ti)O3 lead-free piezoelectric ceramics – the critical role of processing on properties', Journal of the European Ceramic Society, vol. 35, no. 13, pp. 3445-3456. https://doi.org/10.1016/j.jeurceramsoc.2015.05.010

$(Ba,Ca)(Zr,Ti)O_3$ Lead-free Piezoelectric Ceramics – The Critical Role of Processing on Properties

Yang Bai[a,b]*, Ales Matousek[a], Pavel Tofel[a], Vijay Bijalwan[a], Bo Nan[a], Hana Hughes[a] and Tim W. Button[a,b]

[a]CEITEC – Central European Institute of Technology, Technicka 3058/10, 61600 Brno, Czech Republic

[b]School of Metallurgy and Materials, University of Birmingham, Birmingham, B15 2TT, United Kingdom

*Email: Yang.Bai@ceitec.vutbr.cz

Abstract

Lead-free piezoelectric compositions based on $(Ba,Ca)(Zr,Ti)O_3$ have been reported to exhibit many piezoelectric properties similar to the conventionally used $Pb(Zr,Ti)O_3$ materials, and have thus been attracting much attention as potential replacements for lead-based piezoceramics. However, there appears quite a wide variation in the reported piezoelectric properties of the BCZT ceramics, indicating that such properties may be sensitive to fabrication and processing methods. This paper reports an investigation of a wide range of processing factors, including composition (e.g. ratio of $Ba(Zr,Ti)O_3$ to $(Ba,Ca)TiO_3$), sintering conditions (temperature and cooling rate), particle size of the calcined ceramic powder, structure and microstructure (e.g. phase, lattice parameters, density and grain size), and their effect on the piezoelectric properties. For individual compositions, lattice constants and grain size, which are themselves dependent on the ceramic powder particle size and sintering conditions, have been shown to be very important in terms of optimising piezoelectric properties in these materials.

Keywords: BCZT; lead-free piezoelectric; processing; microstructure; d_{33}

1. Introduction

Lead (Pb), although being a highly toxic element, is widely used in a range of piezoelectric ceramic compositions, e.g. PZT ($PbZr_xTi_{1-x}O_3$), PMN-PT ($PbMg_{1/3}Nb_{2/3}O_3$-$PbTiO_3$) and PZnN-PZT ($PbZn_{1/3}Nb_{2/3}O_3$-PZT). However, driven by impending environmental legislation, there is now an urgent need to develop environmentally friendly piezoelectrics[1] where the lead content is much reduced or, preferably, eliminated. As a result, a number of lead-free perovskite piezoelectric materials, such as BNT-BT ($Bi_{1/2}Na_{1/2}TiO_3$-$BaTiO_3$), KNN ($K_{1-x}Na_xNbO_3$), BCZT ($(Ba,Ca)(Zr,Ti)O_3$) and their doped counterparts, have received considerable attention in recent years because of their environmental friendliness, and their good piezoelectric properties (e.g. piezoelectric charge coefficient d_{33} of 200-600 pC/N, coupling coefficient k_p of 0.3-0.5) which are similar to conventionally used hard or soft PZT[1, 2, 3, 4, 5, 6]. Also, BNT-BT and KNN based compositions exhibit high Curie temperatures (T_c =200-400 °C)[2], which, together with the above characteristics, has made them promising candidates to replace conventional PZT for applications of sensors, actuators and transducers. For example, textured KNN ceramic doped with $LiTaO_3$ and $LiSbO_3$ have been reported to exhibit d_{33} values ~416 pC/N and a T_c of 253 °C[7], and d_{33}, k_p and T_c values of ~425 pC/N, 0.5 and ~200 °C respectively have been reported for a KNN-$BaZrO_3$ composition doped by Li and Sb at the rhombohedral-tetragonal morphotropic phase boundary (MPB)[5]. In addition, a series of alkaline-niobate based systems have been made with good piezoelectric properties, e.g. d_{33} values between 390-490 pC/N and T_c 217-304 °C.

One particular milestone of the development of lead-free piezoelectrics could be considered to be the reports of extremely high d_{33} values in a solid solution of $(1-x)Ba(Zr_{0.2}Ti_{0.8})O_3$-$x(Ba_{0.7}Ca_{0.3})TiO_3$ (1-xBZT-xBCT) with a peak value about 620 pC/N at the x=0.5 composition[4], even higher than that of a 'soft' PZT[3, 7]. Particular features of the BZT-BCT system are the strongly curved Morphotropic Phase Boundary (MPB)[4] between rhomboheral BZT and tetragonal BCT structures, and also its

sensitivity to processing and fabrication method. The piezoelectric properties of 0.5BZT-0.5BCT ceramics are reported to be affected by powder synthesis method[4, 8], optimisation of sintering[9, 10], poling conditions[11, 12] and measurement environment[4, 13]. For example, an increase of sintering temperature from 1300 °C to 1500 °C for ceramics of composition $(Ba_{0.85}Ca_{0.15})(Zr_{0.1}Ti_{0.9})O_3$ resulted in an increased density and increased average grain size as well as improved piezoelectric properties, a peak d_{33} value of 442 pC/N being reported for samples sintered at 1440 °C[14]. Also, with addition of an appropriate amount of ZnO, the tricritical point (cubic-rhombohedral-tetragonal phase boundary) of $(Ba_{0.85}Ca_{0.15})(Zr_{0.1}Ti_{0.9})O_3$ was moved to around room temperature, thus inducing an improved d_{33} value of 521 pC/N and k_p of 0.48[15]. In addition, it has been reported that the piezoelectric properties (e.g. d_{33}, k_p) of $(Ba_{0.85}Ca_{0.15})(Zr,Ti)O_3$ ceramics could be maximised by tailoring the Zr/Ti ratio towards 0.1/0.9 where two ferroelectric phases co-existed and by using optimised poling conditions (temperature 40 °C) and electric field 4 kV/mm)[16].

In terms of synthesis methods,, Liu and Ren[4] used an uncommon way to synthesise the BCZT powder, whereby $BaZrO_3$ powder was made initially and then mixed and reacted with other starting materials ($BaCO_3$, $CaCO_3$ and TiO_2) to the required stoichiometry. The calcination and sintering temperatures used in this process were relatively high at 1350 °C and 1450-1500 °C respectively, and they obtained d_{33} values of 560-620 pC/N[4], which have been the highest reported values for this composition to date. Other researchers have used a more conventional way of mixing all the starting materials ($BaCO_3$, $CaCO_3$, TiO_2 and ZrO_2) together and reacting them, but the reported piezoelectric properties have been rather variable (d_{33} from 280 pC/N to 570 pC/N)[9, 10, 11, 17, 18]. However, Tian et al.[12], using a conventional solid state powder synthesis method as mentioned above but with lower calcination and sintering temperatures (1200 °C and 1400-1420 °C respectively), obtained a d_{33} value of about 570 pC/N, close to those reported by Liu and Ren.

In addition, Li et al.[11] reported that increasing the poling temperature to the phase transition regions of the 0.5BZT-0.5BCT composition was able to improve the d_{33} values, especially when the poling voltage was applied above the Curie temperature and kept on during cooling. Also, as the MPB is curved around room temperature for the 0.5BZT-0.5BCT composition, even a variation of environmental temperature during measurement could lead to a slight move away from the MPB and hence lead to a decrease in the measured d_{33} value.

Although the measured piezoelectric properties of the BCZT piezoelectric ceramics seem to be rather sensitive to processing, there has been a paucity of published research concerned with establishing the relationships between processing, microstructure and properties. Microstructural features such as grain size and porosity will have a direct influence on material properties[19, 20], and these will be determined by the overall fabrication process. As a first step to understand these complex interdependencies, this paper reports the effects of fabrication parameters (e.g. sintering procedure and powder particle size) on the microstructure, structure and piezoelectric properties (e.g. grain size, density, phase and lattice parameters, d_{33}) for a wide range of compositions of the (1-x)BZT-xBCT pseudo-solid solution system ($0.3 \leq x \leq 0.9$). Also, as the centre composition at x=0.5 has been considered the most attractive for industrial applications, there is particular emphasis on this composition, in order to contribute to the development of a fabrication standard for BCZT piezoelectrics.

2. Experimental

Powders with compositions of 0.1BZT-0.9BCT (1/9 BCZT), 0.3BZT-0.7BCT (3/7 BCZT), 0.4BZT-0.6BCT (4/6 BCZT), 5/5BCZT, 0.6BZT-0.4BCT (6/4 BCZT) and 0.7BZT-0.3BCT (7/3 BCZT) were prepared by solid state reaction, mixing and calcining stoichiometric quantities of $BaCO_3$ (>99.5%, Dakram, UK), $CaCO_3$ (PA, Lachner, CZE), TiO_2 (>99.5%, Dakram, UK) and ZrO_2 (>99.5%, Dakram, UK) powders. The mixing was carried out in distilled water on a horizontal ball mill with ZrO_2 balls for 24 hours, followed by drying at 90 °C for 24 hours. The mixed powders were then calcined at

1100 °C for 4 hours, followed by further horizontal ball milling with ZrO_2 balls and distilled water to yield a calcined powder with an average particle size (D_{50}) of about 5 µm. In order to obtain powders with different particle sizes so that their effects on material microstructures and piezoelectric properties could be investigated, vibratory milling and planetary milling were applied on portions of the calcined 5/5 BCZT powder, resulting in reductions in D_{50} to about 3 µm and 1 µm, respectively. The milled powders were then mixed with 10 wt% of a combination of two types of water-based PVA binder (Duramax B-1000 and B-1007, Chesham Chemicals Ltd., UK), and unixially pressed at 148 MPa into disc-shaped green bodies with diameter of 13 mm and thickness under 1 mm. The green bodies were subsequently sintered at selected temperatures between 1300-1525 °C for 4 hours in air, with heating and cooling rates of 5 °C/min. 1 hour dwells at 350 °C and 500 °C were included during the heating cycle in order to burn off the binders. Some samples were also subjected to a slower cooling rate (1 °C/min). Au-Cr electrodes were sputtered on both sides of the sintered discs. Finally, all samples were poled at room temperature (20-25 °C) in a silicone oil bath under a DC electric field of 3 kV/mm for 10 minutes.

The particle sizes of the calcined and milled ceramic powders were measured using a particle size analyser (Gracell, Sympa Tec, Germany). The densities of all the sintered ceramic samples were calculated by the Archimedes method, and then expressed as a percentage of the theoretical density (defined as relative density) using theoretical values calculated from the X-ray diffraction (XRD) data. The theoretical density of each BCZT composition was calculated according to the atomic weight and unit cell lattice parameters from XRD, and assuming the sintered ceramics were fully dense. XRD (SmartLab, Rigaku, Japan) was used to identify the phases present and their lattice parameters, and sintered grain sizes were obtained using the linear intercept method[21] on scanning electron micrographs (SEM, Ultra Plus, Zeiss, USA) of polished samples which had been thermally etched for 10 mins at a temperature 100 °C below the sintering temperature. The d_{33} values of the poled samples were measured by a Berlincourt d_{33} meter (YE2730A, Sinocera, China), and ferroelectric hysteresis loops (P-E loops) of selected samples were measured using a Piezoelectric Evaluation System (AixPES, Aixacct, Germany). The temperature dependence of the dielectric properties (relative permittivity and dielectric loss factor) were characterised using an impedance analyser (4194A, Hewlett Packard, USA) and an environmental chamber (TJR, Tenny Environmental-SPX, USA).

3. Results and Discussion

3.1. Effects of Sintering on Grain Size and Density

The effect of sintering temperature on the relative density and grain size of samples with different compositions and fabricated from 5 µm powders is shown in Fig. 1, where sintering was carried out with the normal cooling rate of 5 °C /min

All of the samples achieved greater than 90 % relative density, which suggested that sintering temperatures of 1400-1500 °C were sufficient for the 5 µm BCZT powders to produce good quality ceramics. However, it is noticeable that the sintered grain sizes were between 10-50 µm for the samples with compositions of 1/9, 3/7, 4/6, 5/5 and 6/4 BCZT and >60 µm for those of the 7/3 BCZT composition. These values are much larger than the typical values of around 1-5 µm for PZT ceramics[22, 23], and indicates that the grain growth of the BZT-BCT pseudo-solid solution might follow a similar pattern to that of $BaTiO_3$ where rapid grain growth is a well-established phenonenon[19, 24]. It can also be seen that the relationship between sintering temperature and density or grain size is different for each composition. For the 1/9, 3/7 and 7/3 samples (see Fig. 1 (a)(b)(f)), maximum density was achieved in samples sintered at 1475 °C. However, for the 5/5 composition (see Fig. 1 (d)) density continued to increase up to 1500 °C, and for the 4/6 and 6/4 compositions (see Fig. 1 (c)(e)) maximum densities were achieved at lower sintering temperatures. For the 6/4 composition samples a density minimum was observed at 1475 °C with densities increasing again up to a sintering temperature of 1525 °C (see Fig. 1 (e)).

The variation in grain size with sintering temperature is more complex to summarise. Such a phenomenon of irregular density and grain size trend might imply an unusual densification and grain growth mechanism for the different compositions, but such a discussion is beyond the scope of this paper. However, the observed behaviour does enable samples with a broad range of different average grain sizes to be prepared as was required to support the subsequent investigation on relationships between grain size and piezoelectric properties.

The effect of lowering the cooling rate from 5 to 1 °C/min during the sintering process was investigated for the 1/9, 3/7 and 5/5 BCZT composition samples sintered at 1475 °C, and the effects of this on the relative density and grain size are shown in Fig. 2, and compared to values obtained using the normal cooling rate.

It can be seen that the implementation of a slower cooling rate always increased the relative density of all compositions by 2-3 % (see Fig. 2 (a)). This could be expected due to the increased overall time at high temperatures experienced by the samples. However, the effect on grain size was dependent on sample composition (see Fig. 2 (b)). For the 1/9 BCZT samples, slow cooling led to approximately 10 μm smaller average grain size than obtained by normal cooling, whereas for the 5/5 BCZT samples, the average grain size for slow cooled samples became about 10 μm larger. However, for the 3/7 BCZT composition, no obvious difference in grain size with cooling rate was observed. This behaviour may imply that the mechanisms of grain growth for compositions across the BZT-BCT pseudo-solid solution system might vary and, as mentioned above, this may cause a complexity for the investigation of the sintering of BZT-BCT ceramics. However, changes in the cooling rate during sintering could be a supplementary method used to obtain specific samples with different average grain sizes, providing further support to the subsequent investigation on relationships between grain size and piezoelectric properties.

3.2. Effects of Particle Size on Sintering Behaviour and Grain Growth

It is well-known that powder particle size can have a major influence on the sintering behaviour of ceramics, with smaller particle size, higher surface area powders usually sintering more quickly and enabling the use of lower sintering temperatures[25]. Hence, in this study, the effects of particle size of the calcined ceramic powder on sintering behaviour, microstructure and final piezoelectric properties of samples of the 5/5BCZT composition have also been investigated. The variation of relative density and grain size with sintering temperature for 5/5 BCZT samples made from ceramic powders with D_{50} particle sizes of 5, 3 and 1 μm are shown in Fig. 3.

As would be expected, the use of smaller powder particles enables densification to be achieved at lower sintering temperatures. For example, densities >96 % were achieved in samples made from the 1 μm powder sintered at 1300-1350 °C, while sintering temperatures of 1425-1450 °C and 1500 °C are required for samples made from the 3 μm and 5 μm powders, respectively, in order to achieve the same level of densification (see Fig. 3 (a)). The density of samples prepared from the 1 μm powder decreased with an increase of sintering temperature (see Fig. 3 (a)). As significant densification was achieved at a sintering temperature of 1300 °C, a contributing factor in achieving lower densities for higher sintering temperatures could be that grain growth started to take place before densification was completed (see Fig. 3 (b)), possibly leading to trapped porosity. Similarly, the maximum densification of samples produced from the 3 μm powder was achieved at a sintering temperature of 1425 °C with a corresponding grain size of approximately 20 μm. At higher sintering temperatures the grain size increased (see Fig. 3 (b)) and density decreased (see Fig. 3 (a)). For the samples produced from the 5 μm powder, densification and grain growth increased together over the more limited range of sintering temperatures that were investigated, the slower densification behaviour possibility being dominated by use of the larger particle size powder with surface lower surface area.

It is interesting to see that for sintering temperatures ≥1400 °C smaller powder particle size resulted in larger sintered grain size (see Fig. 3 (b)). For example, the average grain sizes of the samples made from the 1 µm, 3 µm and 5 µm powders and sintered at 1450 °C were about 20 µm, 35 µm and 55 µm, respectively. Example microstructures of sintered and thermally etched samples fabricated from 1, 3 and 5 µm powders are shown in Figs. 4, 5 and 6, respectively. Although it has been reported previously that increased grain size tended to induce improved piezoelectric properties[14], a broader investigation is reported here and a discussion about the effects of grain size and other structural factors on piezoelectric properties is presented in sections 3.4 and 3.5.

3.3 Effects of Composition on Dielectric Properties

The temperature dependence of relative permittivity (ε_r) and dielectric loss factor ($tan\delta$) for the samples of each composition sintered at 1475 °C are shown in Fig. 7. All samples were produced using powders with a particle size of 5 µm. The phase transition regions for each composition were taken to be when the peaks (or gradient changes) of the relative permittivity and dielectric loss factor could be observed at the same temperature. It can be seen that the 1/9 and 7/3 compositions exhibited only one phase transition in the range of -50 to 130 °C at 100-120 °C, 110-130 °C and 55-75 °C respectively. These phase transitions are indicative of the Curie temperature for each composition and are consistent with those in the literature[4, 8, 26]. However, for the 4/6, 5/5 and 6/4 compositions, more than one phase transition is observed in the measured temperature range. A draft of phase diagram has been plotted using the phase transition temperatures observed in Fig. 7, and is shown in Fig. 8.

It can be seen that the phase diagram in Fig. 8 is rather similar to that first reported by Liu and Ren[4], where a curved MPB sits between the rhombohedral and tetragonal phases and a tricritical point is found near the composition of 7/3 BCZT at about 60 °C, and thus the cubic, tetragonal and rhombohedral phase fields have been tentatively marked on the diagram. Some recent reports[12, 26] have proposed the existence of an additional phase region between the rhombohedral and tetragonal phases. Such a phase region can also be observed in Fig. 8 (marked as phase γ) which could therefore be tentatively defined as an orthorhombic[12, 26] phase region, as found in the parent $BaTiO_3$ composition. The definition of such a phase diagram (Fig. 8) is crucial in order to explain and understand the relationships of material processing, microstructure and electrical properties, and further work in this area is planned. It can be expected that a composition falling on the boundary between two ferroelectric phases (i.e. an MPB) should have good poled piezoelectric properties, as more domain orientations would be allowed in these regions.

3.4 The Effect of Sintering and Particle Size on Structure and Lattice Parameters

Different sintering temperatures may not only affect densification and grain growth, but also alter the structural phases present in the sintered ceramics and their lattice parameters. Thus, the effects of sintering and powder particle size on the structural phases and lattice parameters of the 1/9, 3/7, 4/6, 5/5, 6/4 and 7/3 BCZT compositions were also investigated. The XRD patterns obtained at room temperature of the 4/6 BCZT samples sintered at 1425, 1475 and 1525 °C are shown in Fig. 9.

All of the XRD patterns corresponded to perovskite-type structures, with the tetragonal modification identified as the dominant phase in all of the samples. Evidence for this can be seen by the splitting of the (001)/(100) and (002)/(200) peaks (Fig. 9 (1) and (4)), as well as the single peak of for the (111) reflection (Fig. 9 (3)). The only other peaks correspond to the $K\alpha_2$ wavelength of the X-ray source used (marked in Fig. 9 (3) and (4)), and reflections from the sample holder. This is consistent with the phase transition behaviour shown in Fig. 7 (b) and the phase diagram presented in Fig. 8, where the 4/6 BCZT composition is in a tetragonal phase region at room temperature. It can also be seen that for the samples sintered at different temperatures, there are only very small differences of the peak positions, intensities and shapes, even in the magnified sections of individual peaks (see Fig. 9 (1)(2)(3)(4)). The lattice parameters of the corresponding structures are listed in Table 1 where it can

be seen that although the values of lattice parameter of the samples sintered at different temperatures were slightly different, the *c*/*a* ratios were identical.

The effects of both sintering temperature and calcined powder particle size on the structures and lattice parameters of the 5/5 BCZT samples are shown in Fig. 10 and Table 2.

Again, it can be seen that the tetragonal modification of the perovskite structure was identified as the majority phase present in all of the 5/5 BCZT samples made from 1 μm or 5 μm powder and sintered at 1325 °C or 1500 °C. However, as the shapes of the peaks labelled as $K\alpha_2$ in Fig. 10 (3) and (4) vary with processing conditions, unlike those labelled in Fig. 10 (3) and (4), it is likely that the orthorhombic phase is also present. The identification of more than one phase is consistent with the phase transition behaviour shown in Fig. 7 (c) and the phase diagram shown in Fig. 8, where the 5/5 BCZT composition at room temperature falls in the region of the MPB of orthorhombic and tetragonal phases. The lattice parameters of tetragonal phase are given in Table 2. Comparing the samples made from the same powder (1 μm) but sintered at different temperatures (1325 °C and 1500 °C), the XRD patterns appear extremely similar to each other (see Fig. 10 a* and b*). The only differences were found on the specific lattice parameters as listed in Table 2, resulting in a slightly larger *c*/*a* ratio for the sample sintered at 1325 °C compared to that sintered at 1500 °C. However, when comparing the samples sintered at the same temperature (1500 °C) but made from powders of different size (1 μm and 5 μm), more significant differences were observed on the XRD patterns (see Fig. 10 b* and c*), especially for some characteristic peaks as highlighted in Fig. 10 (1)(2)(3)(4). In particular, a separate peak corresponding to the (002) tetragonal can be observed on pattern c* in Fig. 10 (4), implying a more significant co-existence of the orthorhombic and tetragonal phases. As a result, notably larger *c*/*a* ratios for the samples prepared with the 5 μm powder compared to those prepared with the 1 μm powder were measured, as shown in Table 2.

The variation in the *c*/*a* ratios of the tetragonal phases identified in samples of the 1/9, 3/7, 4/6 and 5/5 BCZT composition fabricated from 5 μm powders and sintered at 1475 °C are shown in Fig. 11. Samples from the 6/4 and 7/3 BCZT samples were identified as having rhombohedral structures so are not included. It can be seen that there is a small but distinct linear reduction in *c*/*a* as the Ca content deceases. A variation in lattice parameter with composition is to be expected due to the different ionic sizes of the constituent cations. This has been observed for the BCT system[27] where both the *c* and *a* parameters decreased with increasing Ca content, but the resulting *c*/*a* ratio was approximately independent of Ca content with a value of 1.009 in the same Ca composition range. However, in the BCZT system investigated in this work, an increase in the Ba^{2+}/Ca^{2+} ratio is accompanied by a decrease in the Ti^{4+}/Zr^{4+} ratio, thus involving more complex changes in both the A and B sites of the perovskite lattice. The reported *c*/*a* ratio of the $Ba(Zr_{0.2}Ti_{0.8})O_3$ (the end composition without Ca^{2+} in this paper) powder made by a sol-gel process is 1.0011 (tetragonal phase)[28], whereas the largest *c*/*a* ratio of 1.009 achieved by the 1/9 BCZT sample in Fig. 11 is close to the reported datum of 1.01 (tetragonal phase) for the parent composition $BaTiO_3$[29].

Summarising the results from the structural investigations, it would appear that, for any particular BZT-BCT composition, as long as the samples were sintered into well densified ceramics (with > 90 % relative density, see Fig. 1 (c) and (d)), sintering temperature does not affect the crystal structures or lattice parameters (e.g. *c*/*a* ratio). However, although particle size is not likely to be a driving force to alter crystal structures, it might have effects on the specific lattice parameters and resulting *c*/*a* ratios. The composition also has an obvious influence on the *c*/*a* ratio. In principle, the *c*/*a* ratio is a factor describing the anisotropy of tetragonal perovskite unit cells, which should be related to ferroelectric/piezoelectric response (e.g. remanent polarization and d_{33}), and this is explored in the next section.

3.5 Effects of Microstructure on Piezoelectric Properties

In an effort to correlate the microstructures of the BZT-BCT ceramics with their piezoelectric properties, and thus further define the influence of processing, the relative density, average grain size, average *c*/*a* ratio, structures, corresponding d_{33} values and brief sintering procedures of samples of the 1/9, 3/7, 4/6, 5/5, 6/4 and 7/3 BCZT compositions made from 5 μm powders are listed in Table 3.

All of the samples achieved a relative density >87 %, and the measured values of the *c/a* ratios were grouped according to composition. It can also be seen that although having the smallest *c*/*a* ratios, the 5/5 samples generally exhibited higher d_{33} values than the other samples. This was because the BZT-BCT system exhibits an MPB at the 5/5 composition around room temperature, allowing active phase transitions and thus more potential polarisation orientations.

For a particular composition the sintered grain size seemed to have a more significant influence on the d_{33} values than density. For example, the d_{33} values of the 4/6 samples increased from 250 pC/N to 299 pC/N as the average grain size increased from 13.6 μm to 36.6 μm. However, the corresponding change in relative density appeared to be more random. A similar trend was observed for the 5/5 samples, where the d_{33} value increased from 301 pC/N to 466 pC/N for a corresponding increase in grain size from 19.4 μm to 31.5 μm. A small further increase in grain size of the 5/5 samples to 33.1 μm resulted in a decrease in d_{33} value to 387 pC/N. This might be a result of a decrease of the relative density (from 96.3 % to 95.6 %), or be an indication of some form of 'grain size threshold' effect, whereby further increases in grain size resulted in the measured d_{33} values remaining constant or even decreasing. It can also be further seen that when samples were sintered to dense ceramics (>90% relative density), density might not be a critical factor affecting the piezoelectric properties such as d_{33}. It was common that a decreased relative density did not result in a corresponding decrease in the d_{33} value, but was seen to increase with increasing average grain size for the samples of 1/9, 3/7, 6/4 and 7/3 BCZT composition. There is also some indication that samples of the 6/4 BCZT composition might also exhibit the 'grain size threshold' or 'plateau' effect introduced above for the samples of 5/5 BCZT composition, with the d_{33} values remaining approximately constant (295 - 289 pC/N) as the average grain size increased from 28.4 μm to 37.8 μm. There was, however, also an associated slight increase in the relative density.

As a summary of Table 3, values of d_{33} were found to be very dependent on the composition, with the maximum value of 466 pC/N for samples of the 5/5 BCZT composition with a relative density of about 96.3 % and an average grain size of 31.5 μm (relating to samples sintered at 1475 °C with a slow cooling rate). This variation in d_{33} with composition is consistent with the published phase diagram for these materials which shows an MPB around the 5/5 BCZT composition. More significantly, for individual compositions, an increase in the average sintered grain size exhibited a primary and mostly positive effect on the d_{33} value.

3.6 Effects of Particle Size, Grain Size, Lattice Parameters and Properties

The variation of d_{33} value with average sintered grain size of the samples of the 5/5 BCZT composition made from powders of different particle size is shown in Fig. 12, together with the *c/a* ranges of the tetragonal phases measured for each group of samples.

Firstly it can be seen in Fig. 12 is that the particle size of the ceramic powder affected the general magnitude of the d_{33} values that were observed. In particular, the d_{33} values of the samples made from the 3 μm and 5 μm powders were in the range of 300-500 pC/N, while those of the samples made from 1 μm powder only reach a peak d_{33} value of 300 pC/N. Such a large difference could be determined by the *c/a* ratios labelled in Fig. 12. As all of the samples were poled and measured under exactly the same conditions, the switching of domains (poling and de-poling) should not be a factor here. However, because the unit cells of the sintered samples produced from the 3 μm and 5 μm powders exhibited larger anisotropy (larger *c*/*a* ratios), the inherent piezoelectric responses might tend to be stronger than those of the samples fabricated from the 1 μm powder in which lower *c/a* ratios were observed. The influence of *c/a* ratio on piezoelectric response of La-doped $Pb(Zr_{0.53}Ti_{0.47})O_3$ has

been discussed[30], where with decreased *c/a* ratio from the optimum point the electromechanical coupling coefficient decreased simultaneously. This may suggest that particle size of calcined powder is likely to be an important factor in processing which could have a considerable effect on the final piezoelectric properties by altering the anisotropy of resulting perovskite unit cells. Recent work on 5/5 BCZT ceramics produced from sol-gel powders[31] has also shown that the tetragonality of the unit cell can influence the piezoelectric properties. However, with samples of similar tetragonality, grain size may also have a significant effect. The ratio of tetragonal to rhombohedral/orthorhombic phases in the samples might affect the piezoelectric properties of the different 5/5 BCZT samples. However, as the experimental and fabrication conditions of the samples with different powder particle sizes were similar, such a factor is not considered dominant. More detailed observation of exact phase structures of the samples of the 5/5 BCZT composition made from different particle size powders requires more advanced analysis methods, e.g. synchrotron radiation.
It can also be seen in Fig. 12 that for each group of samples shown, there is a clear polynomial relationship between the d_{33} value and the average grain size, where the d_{33} value increased with average grain size to a peak, and then decreased as the grain size was increased further. This is considered a so-called 'grain size threshold' effect, first introduced in Section 3.4. The threshold values of 1 μm, 3 μm and 5 μm samples can be predicted as 26 μm, 34 μm and 49 μm, respectively. Such a threshold might be explained by the samples with larger grains being more difficult to be effectively poled. The presence of more domain walls in a single grain could produce a clamping effect or large internal stress, restricting the activity of domain re-orientation and limiting the percentage of switched domains.

The polarisation loops shown in Fig. 13 demonstrate the effect of grain size on the ferroelectric properties (e.g. saturation and remanent polarization) of selected 5/5 BCZT ceramics.

It can be seen that for the samples of the 5/5 BCZT composition made from 5 μm powder, the variations in the average grain size (labelled with arrows) results in a trend in the saturation and remanent polarization similar to that of the d_{33} values (shown in Fig. 8). For example, with an increase of average grain size from 19.4 μm to 31.5 μm, the coercive electric field stayed the same, but the corresponding remanent polarization increased from about 5 μC/cm^2 to approximately 12.5 μC/cm^2. As the average grain size increased further to 33.1 μm, a slight reduction in polarisation was observed. This is additional evidence that the piezoelectric properties of BZT-BCT solid solution system, especially for the centre composition around the MPB, are likely to be sensitively dependent on grain size. A more precisely designed sintering procedure would be also preferred in order to control the grain growth, and thus achieve the highest potential polarization and d_{33} value.

4. Conclusions

The effect of fabrication and processing conditions on the structure, microstructure and properties of ceramics in the lead-free piezoelectric BZT-BCT solid solution system have been studied in detail, and a number of important factors have been identified. Ceramics with a wide range of BZT/BCT compositions have been fabricated using a variety of sintering temperatures and procedures. Well-densified sintered samples have been produced, and the average sintered grain size has been able to be controlled by altering the initial powder particle size, sintering temperature and cooling rate during sintering. However, structural parameters, in particular the *c*/*a* ratios of the tetragonal phase, have been shown to be independent of sintering regime. . A tentative phase diagram has been constructed, based on phase transitions identified by dielectric property measurements, which is consistent with earlier reports.

For particular compositions the piezoelectric properties have been able to be tailored by variations of *c*/*a* ratio of the tetragonal phase and the grain size. Values of d_{33} have been shown to increase with increasing *c*/*a* ratio, while it has been proposed that there is a grain size limit or threshold beyond which the d_{33} values plateau or even begin to decrease.

In order to achieve optimum piezoelectric properties for sintered BZT-BCT ceramics, the following points concerning fabrication and processing are considered critical:

- BZT-BCT compositions should be selected that are close to the MPB region at the working/testing temperature of interest, in order to provide more potential polarization orientations.
- The particle size of the calcined ceramic powder, and possibly the powder synthesis route, should be carefully selected in order maximise *c*/*a* ratios in the sintered ceramics.
- For particular BZT-BCT compositions and powder particle sizes, the sintering procedures should be designed to enable control of grain growth and thus be able to tailor the grain size in the sintered ceramic, in order to optimise properties.

Acknowledgements

The authors gratefully acknowledge the support of the project CEITEC Brno University of Technology – CZ.1.05/1.1.00/02.0068 from ERDF, the Czech Science Foundation under the grant P108/13-09967S, and the SoMoPro II programme. The research leading to these results has acquired a financial grant from the People Programme (Marie Curie action) of the Seventh Framework Programme of EU according to the REA Grant Agreement No. 291782. The research is further co-financed by the South Moravian Region. It reflects only the authors' views and that the Union is not liable for any use that may be made of the information contained therein.

References

1. J. Rodel, W. Jo, K. T. P. Seifert, E. M. Anton, T. Granzow, and D. Damjanovic, "Perspective on the development of lead-free piezoceramics," *Journal of the American Ceramic Society,* 92[6] 1153-77 (2009).
2. P. K. Panda, "Review: environmental friendly lead-free piezoelectric materials," *Journal of Materials Science,* 44[19] 5049-62 (2009).
3. T. R. Shrout and S. J. Zhang, "Lead-free piezoelectric ceramics: Alternatives for PZT?," *Journal of Electroceramics,* 19[1] 113-26 (2007).
4. W. F. Liu and X. B. Ren, "Large piezoelectric effect in Pb-free ceramics," *Physical Review Letters,* 103[25] 257602 (2009).
5. B. Zhang, J. Wu, X. Cheng, X. Wang, D. Xiao, J. Zhu, X. Wang, and X. Lou, "Lead-free Piezoelectrics Based on Potassium–Sodium Niobate with Giant d33," *ACS Applied Materials & Interfaces,* 5[16] 7718-25 (2013).
6. X. Wang, J. Wu, D. Xiao, J. Zhu, X. Cheng, T. Zheng, B. Zhang, X. Lou, and X. Wang, "Giant Piezoelectricity in Potassium–Sodium Niobate Lead-Free Ceramics," *Journal of the American Chemical Society,* 136[7] 2905-10 (2014).
7. Y. Saito, H. Takao, T. Tani, T. Nonoyama, K. Takatori, T. Homma, T. Nagaya, and M. Nakamura, "Lead-free piezoceramics," *Nature,* 432[8013] 84-87 (2004).
8. D. Damjanovic, A. Biancoli, L. Batooli, A. Vahabzadeh, and J. Trodahl, "Elastic, dielectric and piezoelectric anomalies and Raman spectroscopy of 0.5Ba(Ti0.8Zr0.2)O3-0.5(Ba0.7Ca0.4)TiO3," *Applied Physics Letters,* 100[19] 192907 (2012).
9. P. Mishra, Sonia, and P. Kumar, "Effect of sinering temperature on dielectric, piezoelectric and ferroelectric properties of BZT-BCT 50/50 ceramics," *Journal of Alloys and Compounds,* 545 210-15 (2012).
10. M. Jiang, Q. Lin, D. M. Lin, Q. J. Zheng, X. M. Fan, X. C. Wu, H. L. Sun, Y. Wan, and L. Wu, "Effects of MnO2 and sintering temperature on microstructure, ferroelectric, and piezoelectric properties of Ba0.85Ca0.15Ti0.90Zr0.10O3," *Journal of Materials Science,* 48[3] 1035-41 (2013).
11. B. Z. Li, J. E. Blendell, and K. J. Bowman, "Temperature-dependent poling behavior of lead-free BZT-BCT piezoelectrics," *Journal of the American Ceramic Society,* 94[10] 3192-94 (2011).

12. Y. Tian, L. L. Wei, X. L. Chao, Z. H. Liu, and Z. P. Yang, "Phase transition behavior and large piezoelectricity near the morphotropic phase boundary of lead-free (Ba0.85Ca0.15)(Zr0.1Ti0.9)O3 ceramics," *Journal of the American Ceramic Society,* 96[2] 496-502 (2013).
13. M. C. Ehmke, J. Daniels, J. Glaum, M. Hoffman, J. E. Blendell, and K. J. Bowman, "Reduction of the piezoelectric performance in lead-free (1-x)Ba(Zr0.2Ti0.8)O3-x(Ba0.7Ca0.3)TiO3," *Journal of Applied Physics,* 112[11] 114108 (2012).
14. J. Wu, D. Xiao, B. Wu, W. Wu, J. Zhu, Z. Yang, and J. Wang, "Sintering temperature-induced electrical properties of (Ba0.90Ca0.10)(Ti0.85Zr0.15)O3 lead-free ceramics," *Materials Research Bulletin,* 47[5] 1281-84 (2012).
15. J. Wu, D. Xiao, W. Wu, Q. Chen, J. Zhu, Z. Yang, and J. Wang, "Role of room-temperature phase transition in the electrical properties of (Ba, Ca)(Ti, Zr)O3 ceramics," *Scripta Materialia,* 65[9] 771-74 (2011).
16. J. Wu, D. Xiao, W. Wu, Q. Chen, J. Zhu, Z. Yang, and J. Wang, "Composition and poling condition-induced electrical behavior of (Ba0.85Ca0.15)(Ti1−xZrx)O3 lead-free piezoelectric ceramics," *Journal of the European Ceramic Society,* 32[4] 891-98 (2012).
17. W. F. Bai, W. Li, B. Shen, and J. W. Zhai, "Piezoelectric and strain properties of Strontium-doped BZT-BCT lead-free ceramics," in 7th China International Conferences on High-performance Ceramics (CICC 7). Edited by W. Pan and J. H. Gong.
18. C. Han, J. G. Wu, C. H. Pu, S. Qiao, B. Wu, J. G. Zhu, and D. Q. Xiao, "High piezoelectric coefficient of Pr2O3-doped Ba0.85Ca0.15Ti0.90Zr0.10O3 ceramics," *Ceramics International,* 38[8] 6359-63 (2012).
19. Y. Huan, X. H. Wang, J. Fang, and L. T. Li, "Grain size effects on piezoelectric properties and domain structure of BaTiO3 ceramics prepared by two-step sintering," *Journal of the American Ceramic Society,* 96[11] 3369-71 (2013).
20. Y. Hiruma, H. Nagata, and T. Takenaka, "Grain-size effect on electrical properties of (Bi1/2K1/2)TiO3 ceramics," *Japanese Journal of Applied Physics Part 1-Regular Papers Brief Communications & Review Papers,* 46[3A] 1081-84 (2007).
21. M. I. Mendelson, "Average grain size in polycrystalline ceramics," *Journal of the American Ceramic Society,* 52[8] 443-46 (1969).
22. M. J. Hoffmann, M. Hammer, A. Endriss, and D. C. Lupascu, "Correlation between microstructure, strain behavior, and acoustic emission of soft PZT ceramics," *Acta Materialia,* 49[7] 1301-10 (2001).
23. Martiren.Ht and J. C. Burfoot, "Grain-size and pressure effects on dielectric and piezoelectric properties of hot-pressed PZT-5," *Ferroelectrics,* 7[1-4] 151-52 (1974).
24. M. P. McNeal, S. J. Jang, and R. E. Newnham, "The effect of grain and particle size on the microwave properties of barium titanate (BaTiO3)," *Journal of Applied Physics,* 83[6] 3288-97 (1998).
25. C. Herring, "EFFECT OF CHANGE OF SCALE ON SINTERING PHENOMENA," *Journal of Applied Physics,* 21[4] 301-03 (1950).
26. D. S. Keeble, F. Benabdallah, P. A. Thomas, M. Maglione, and J. Kreisel, "Revised structural phase diagram of (Ba0.7Ca0.3TiO3)-(BaZr0.2Ti0.8O3)," *Applied Physics Letters,* 102[9] (2013).
27. D. S. Fu, M. Itoh, and S. Koshihara, "Invariant lattice strain and polarization in BaTiO3-CaTiO3 ferroelectric alloys," *Journal of Physics-Condensed Matter,* 22[5] (2010).
28. C. Thanachayanont, V. Yordsri, S. Kijamnajsuk, N. Binhayeeniyi, and N. Muensit, "Microstructural investigation of sol-gel BZT powders," *Materials Letters,* 82 205-07 (2012).
29. F. D. Morrison, D. C. Sinclair, J. M. S. Skakle, and A. R. West, "Novel doping mechanism for very-high-permittivity barium titanate ceramics," *Journal of the American Ceramic Society,* 81[7] 1957-60 (1998).

30. M. Hammer and M. J. Hoffmann, "Detailed x-ray diffraction analyses and correlation of microstructural and electromechanical properties of La-doped PZT ceramics," *Journal of Electroceramics,* 2[2] 75-83 (1998).
31. K. Castkova, K. Maca, J. Cihlar, H. Hughes, A. Matousek, P. Tofel, Y. Bai, and T. W. Button, "Chemical synthesis, sintering and piezoelectric properties of Ba0.85Ca0.15Zr0.1Ti0.9O3 lead-free ceramics," *Journal of the American Ceramic Society - accepted* (2015).

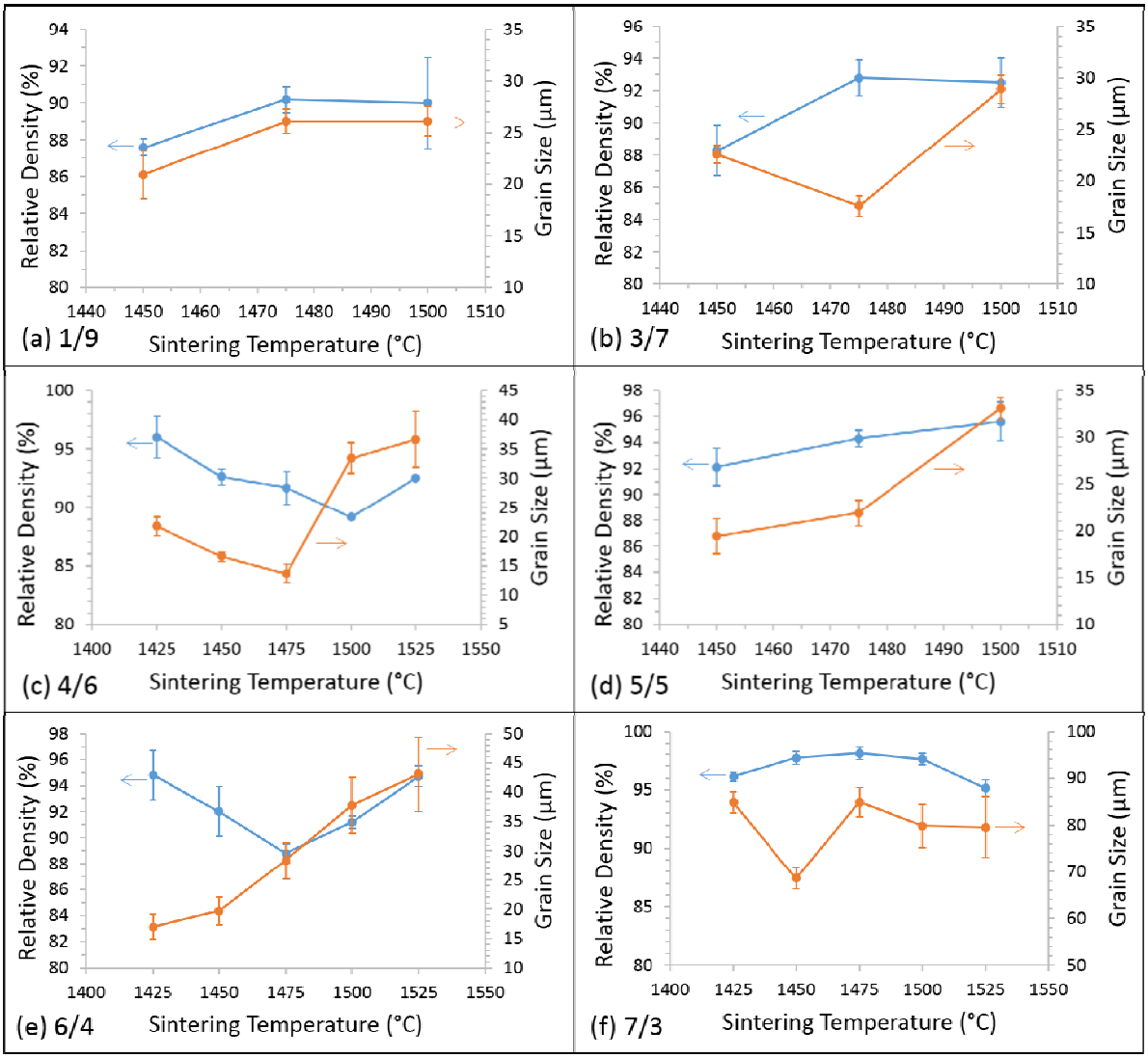

Fig. 1. Dependence of relative density and average grain size on sintering temperature for (a) 1/9 (b) 3/7 (c) 4/6 (d) 5/5 (e) 6/4 (f) 7/3 BCZT ceramics.

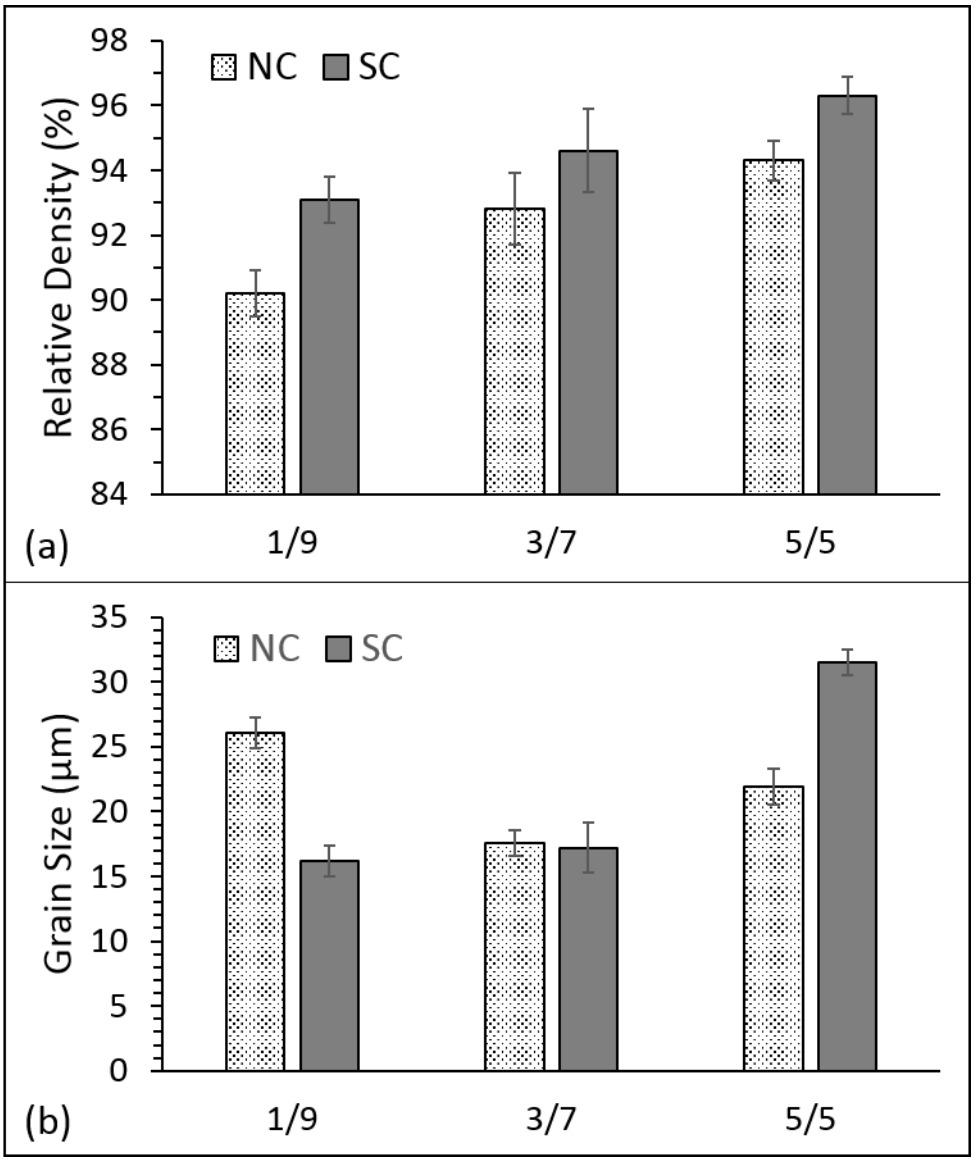

Fig. 2. Comparisons of (a) relative density and (b) average grain size between the samples sintered at 1475 C with normal cooling rate (5 °C/min) and slow cooling rate (1 °C/min) for the 1/9, 3/7 and 5/5 BCZT compositions.

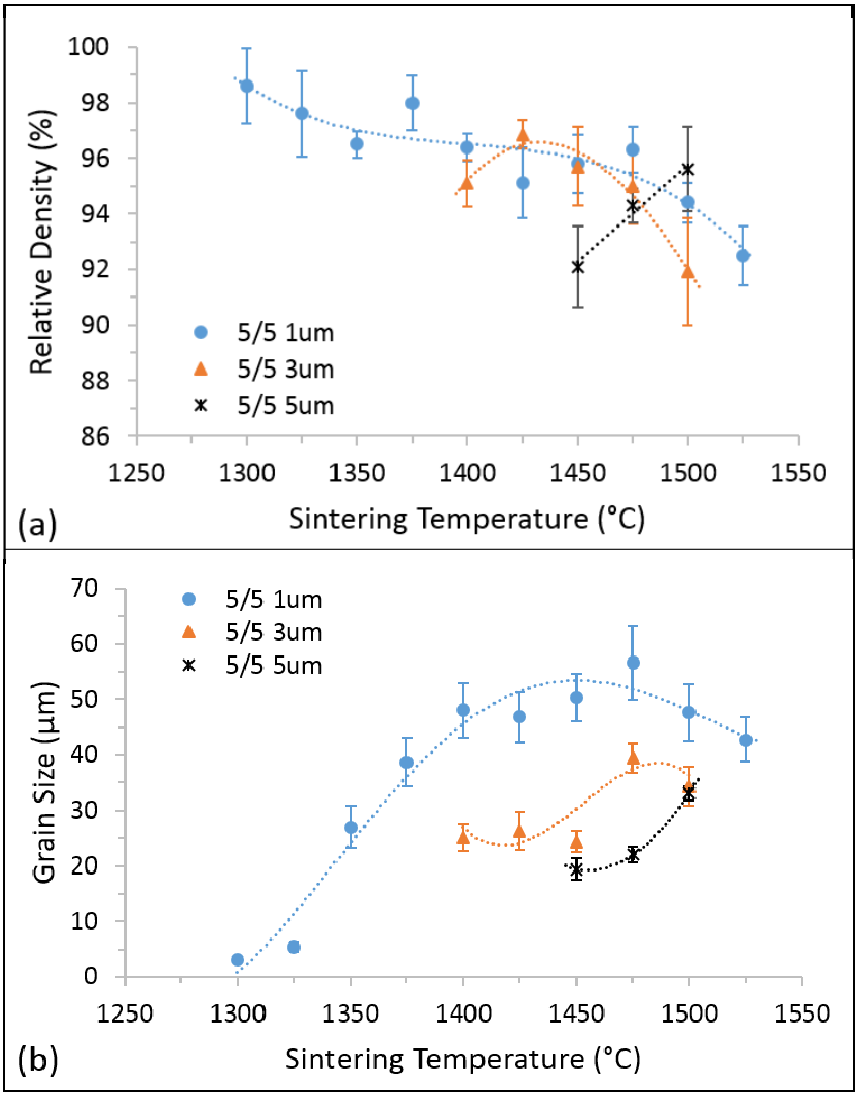

Fig. 3. Dependence of (a) relative density (b) average grain size on sintering temperature for the 5/5 BCZT samples fabricated from ceramic powders of different particle sizes.

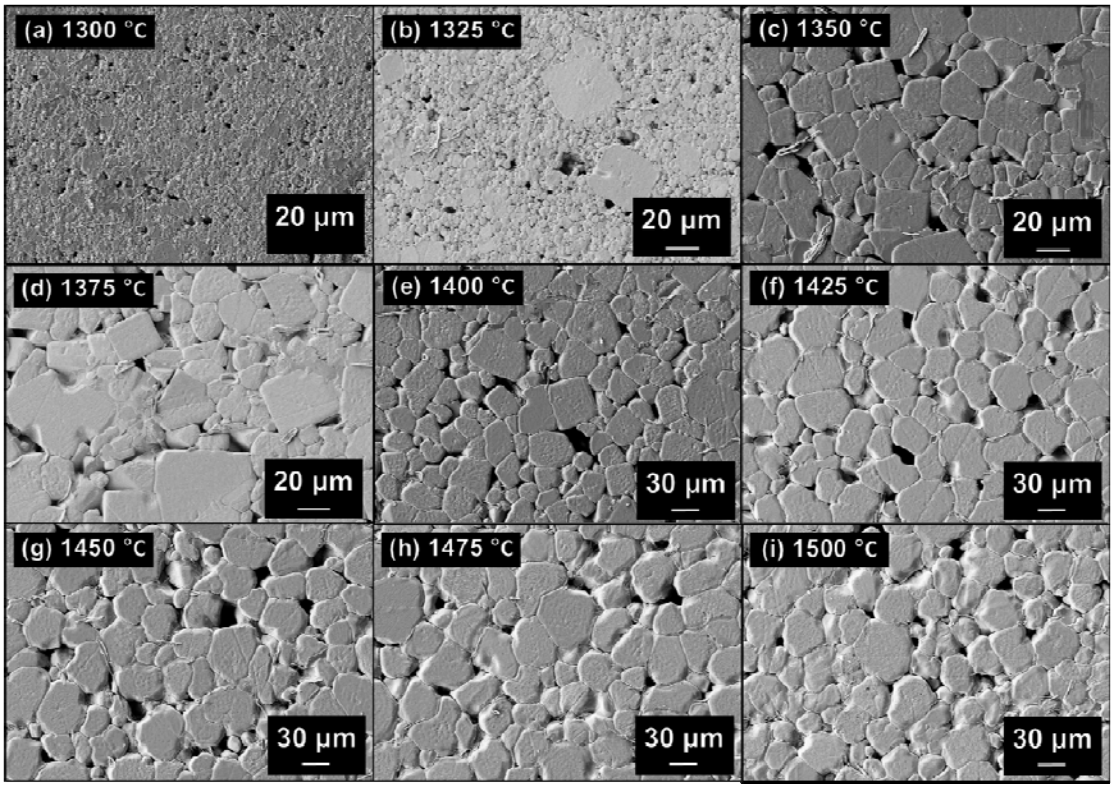

Fig. 4. SEM images of the 5/5 BCZT samples made from 1 µm powder and sintered at temperatures between 1300-1500 °C for 4 hours.

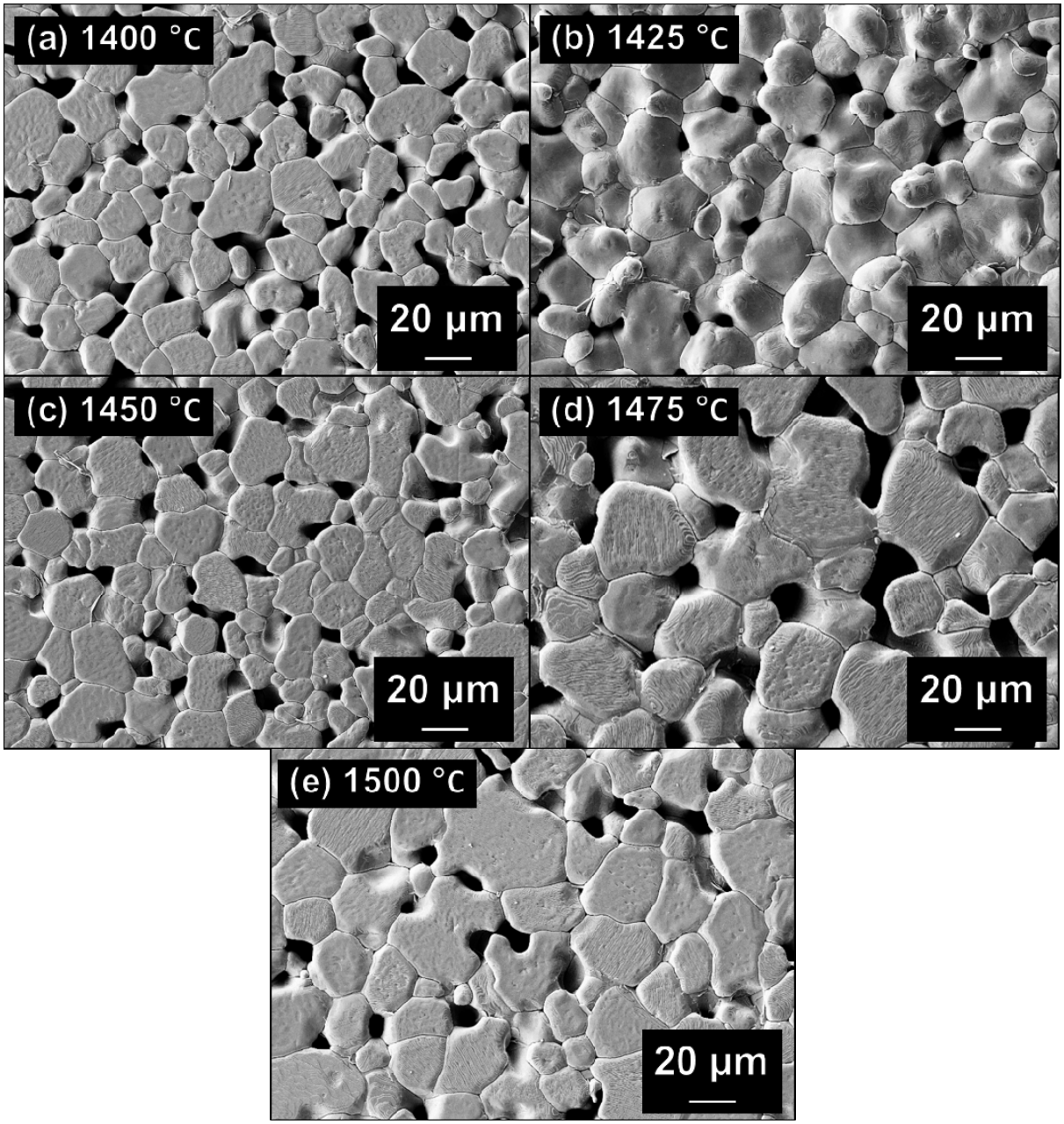

Fig. 5. SEM images of the 5/5 BCZT samples made from 3 µm powder and sintered at 1400-1500 °C for 4 hours.

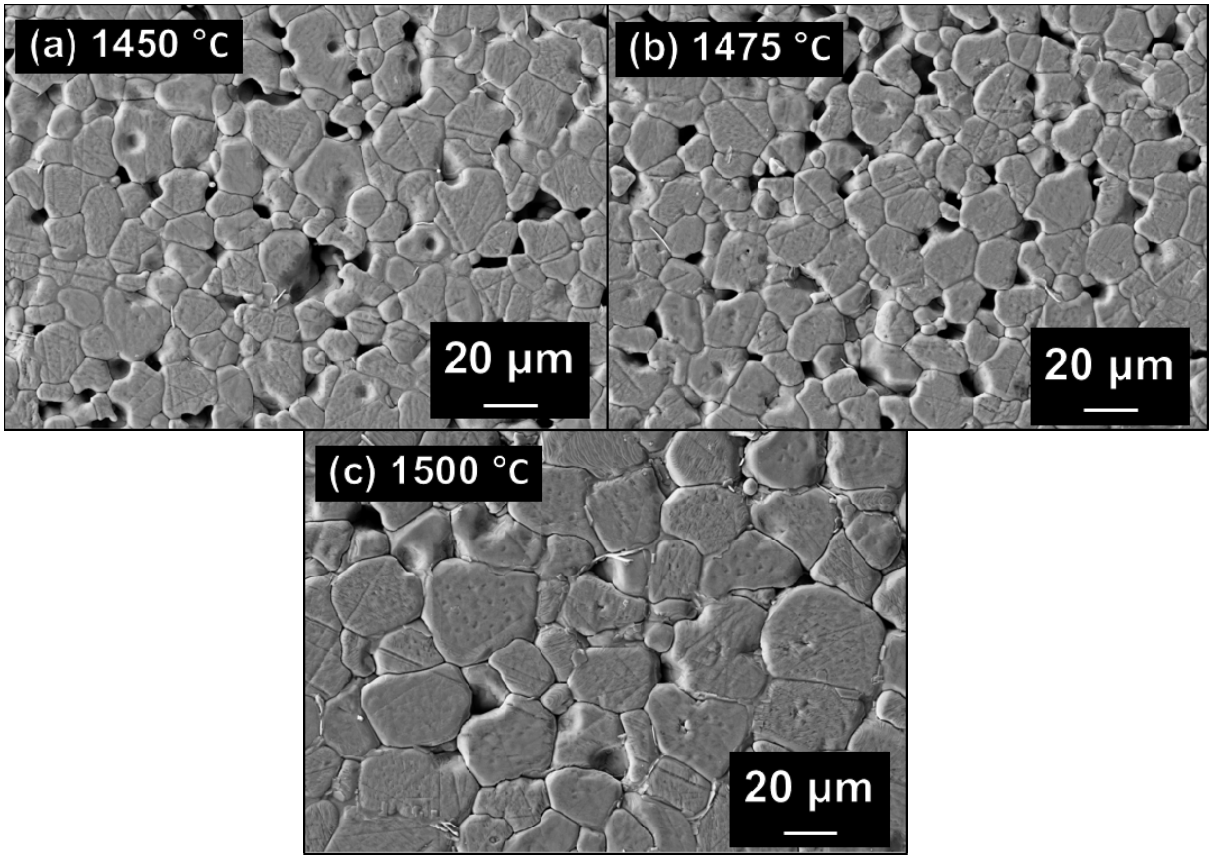

Fig. 6. SEM images of the 5/5 BCZT samples made from 5 µm powder and sintered at 1450-1500 °C for 4 hours.

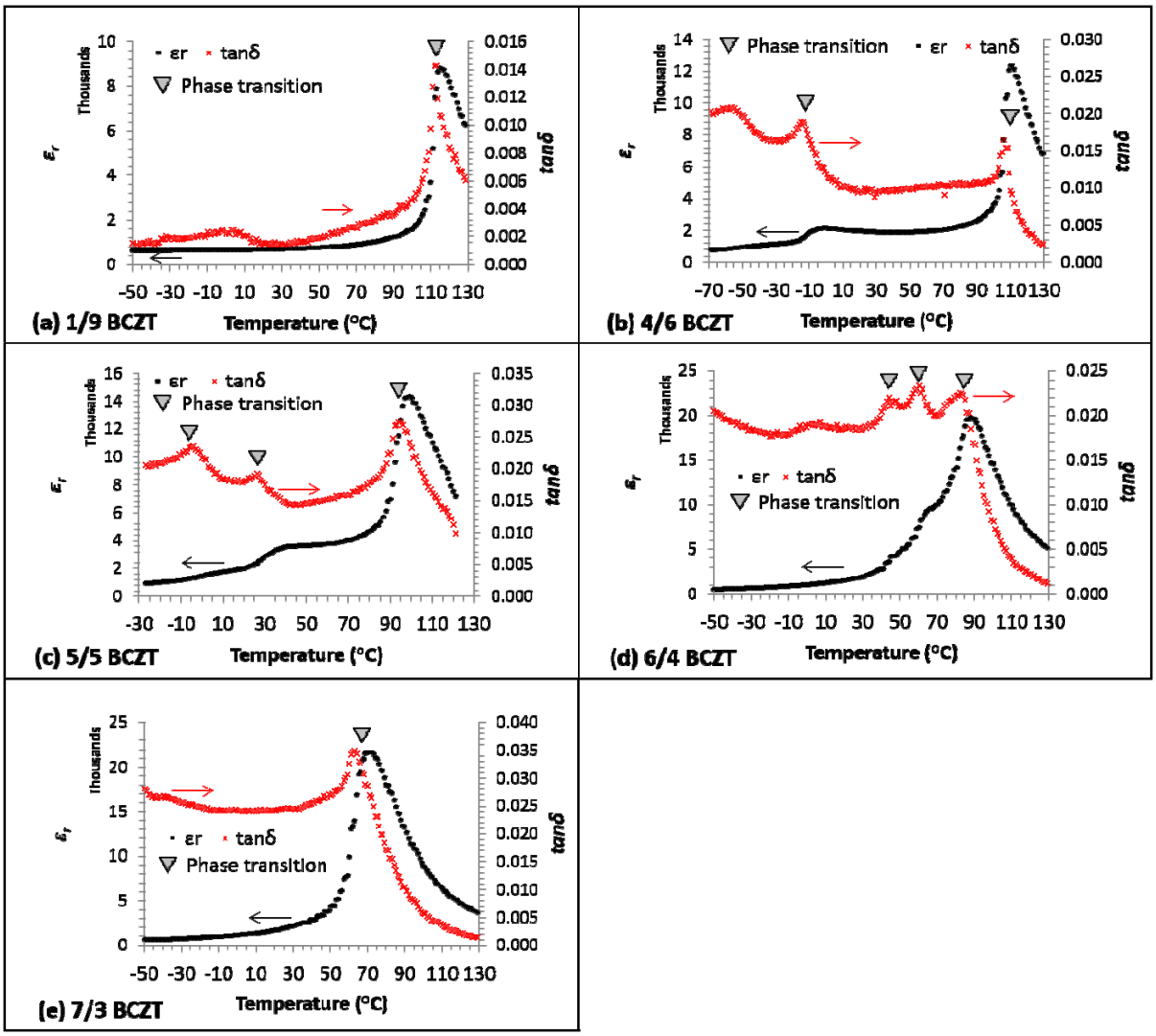

Fig. 7. Dependence of relative permittivity and dielectric loss factor on temperature for the samples of different compositions sintered at 1475 °C with marked phase transitions.

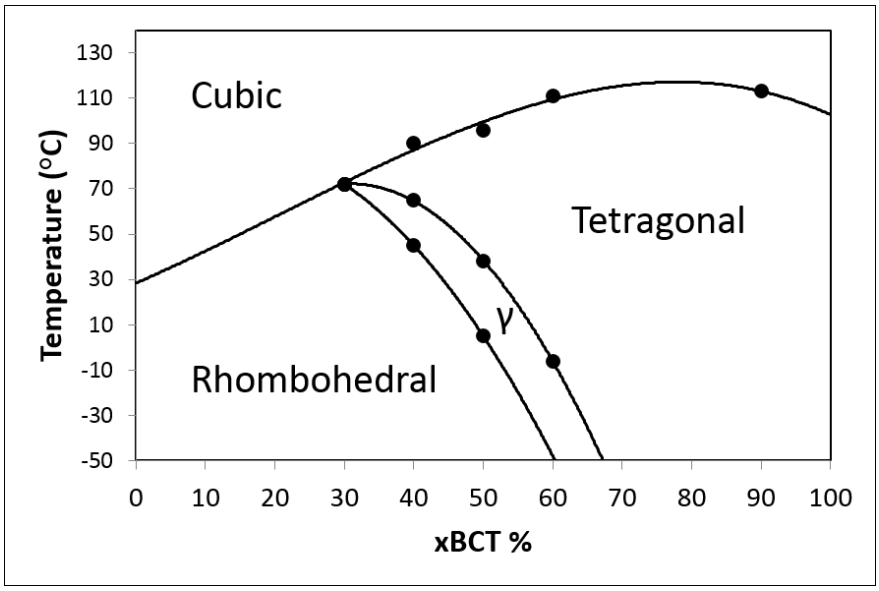

Fig. 8. Tentative Phase diagram of the BZT-BCT solid-solution. Phase regions have been labelled consistent with other published work[4].

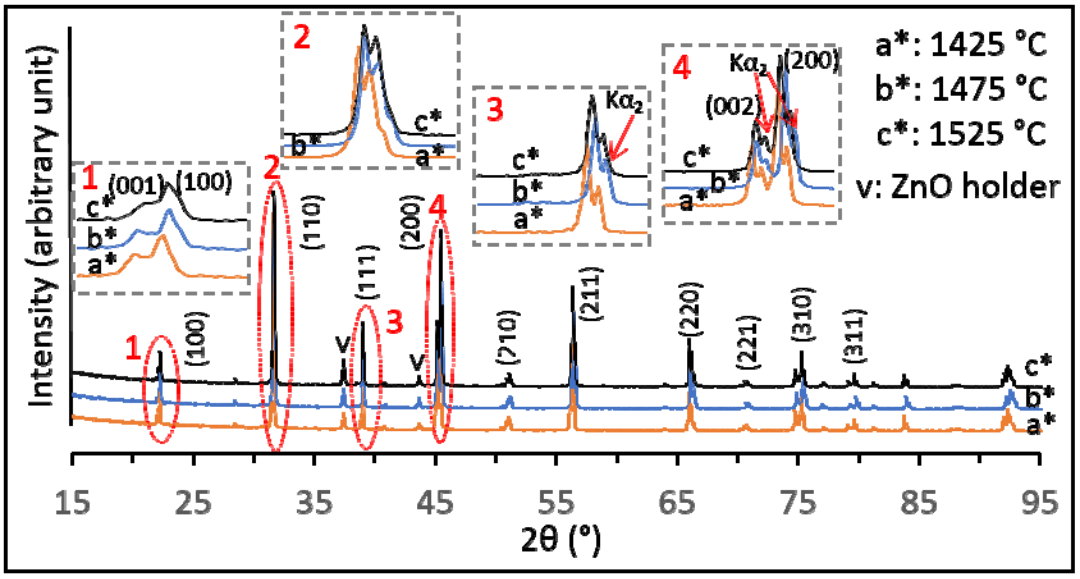

Fig. 9. XRD patterns of the 4/6 BCZT samples fabricated from 5 μm powder and sintered at different temperatures.

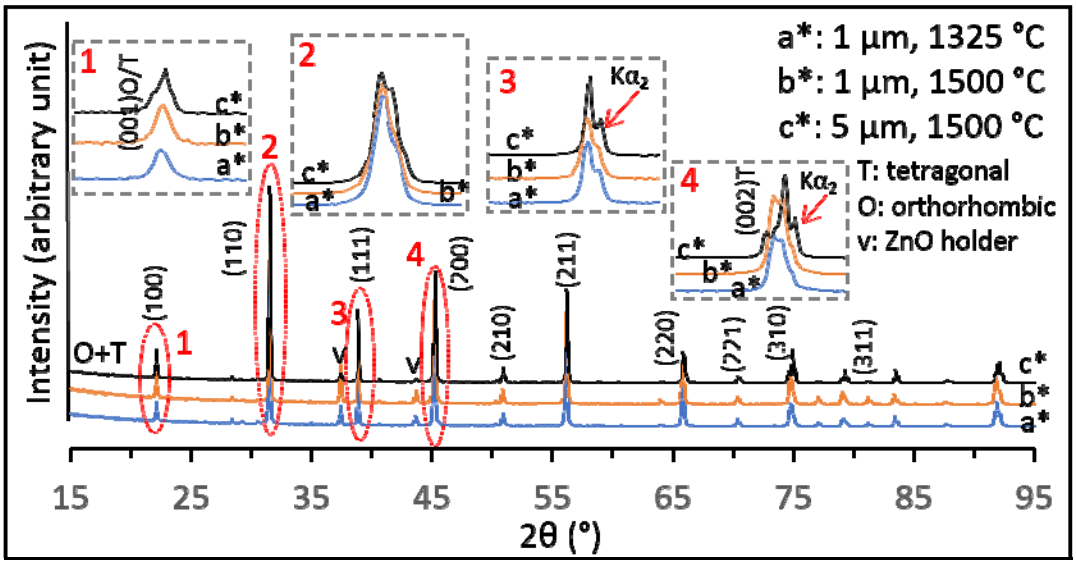

Fig. 10. XRD patterns of the 5/5 BCZT samples made from powders with different particle sizes and sintered at different temperatures.

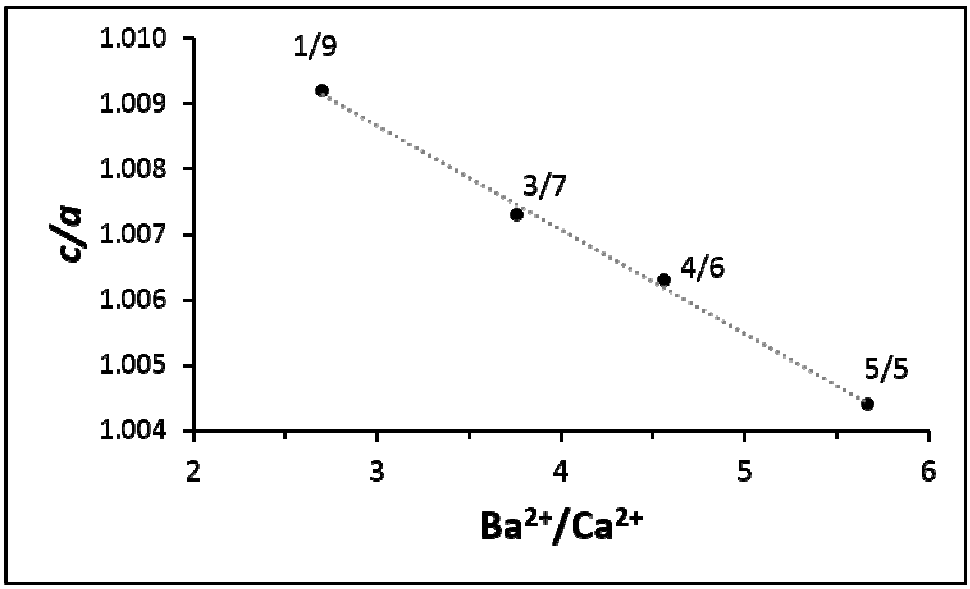

Fig. 11. Dependence of c/a ratio on Ba^{2+}/Ca^{2+} ratio for the tetragonal phases in samples of the 1/9, 3/7, 4/6 and 5/5 BCZT composition fabricated from 5 μm powders and sintered at 1475 °C .

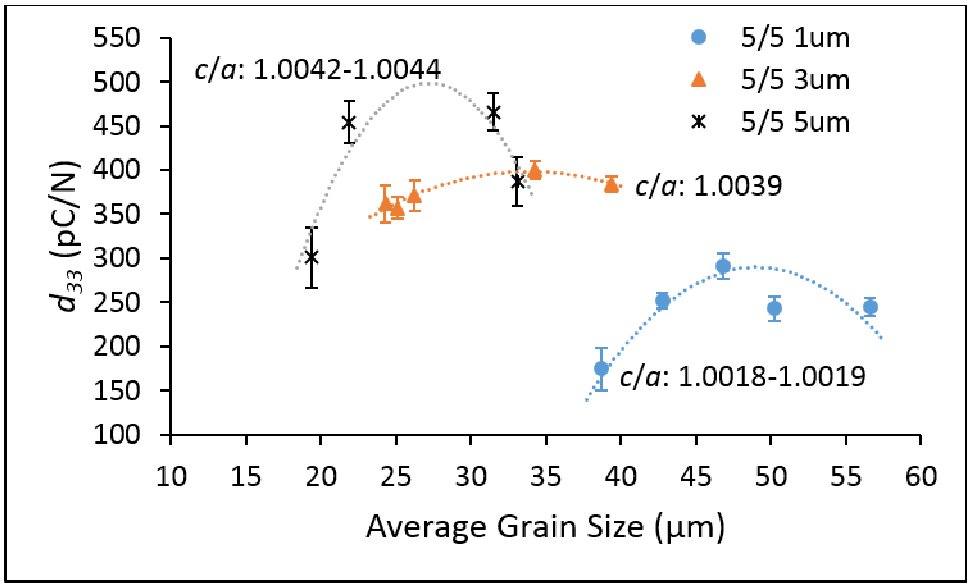

Fig. 12. Dependence of d_{33} value on average grain size for the samples of the 5/5 BCZT composition fabricated from different powder particle sizes.

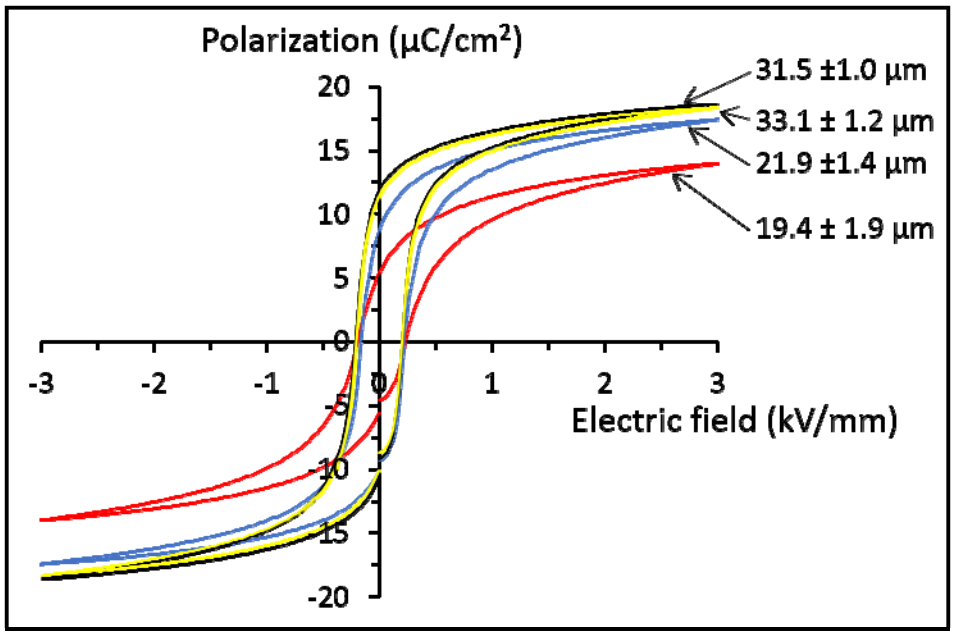

Fig. 13. Dependence of polarization on electric field (P-E hysteresis loop) for the 5/5 BCZT samples with different average grain sizes.

Table 1. Lattice parameters of the 4/6 BCZT samples fabricated with 5 μm powder and sintered at different temperatures.

Sample	Space Group	α (°)	β (°)	γ (°)	a (Å)	b (Å)	c (Å)	c/a
4/6 1425 °C (Fig. 4a*)	P4/mmm	90	90	90	3.9876	3.9876	4.0135	1.0065
4/6 1475 °C (Fig. 4b*)					3.9880	3.9880	4.0132	1.0063
4/6 1525 °C (Fig. 4c*)					3.9890	3.9890	4.0140	1.0063

Table 2. Lattice parameters of tetragonal phase of the 5/5 BCZT samples made from powders with different particle sizes and sintered at different temperatures.

Sample	Space Group	α (°)	β (°)	γ (°)	a (Å)	b (Å)	c (Å)	c/a
1 μm 1325 °C (Fig. 5a*)	P4/mmm	90	90	90	4.0082	4.0082	4.0174	1.0023
1 μm 1500 °C (Fig. 5b*)					4.0093	4.0093	4.0164	1.0018
5 μm 1500 °C (Fig. 5c*)					4.0004	4.0004	4.0174	1.0042

Table 3. Effect of density, grain size, c/a ratio and structures on d_{33} value for samples of 1/9, 3/7, 4/6, 5/5, 6/4 and 7/3 BCZT composition fabricated from 5 um powders, together with relevant sintering procedures.

Sample Composition (BZT/BCT)	Relative Density (%)	Average Grain Size (μm)	Average c/a ratio	Phase Structure	d_{33} (pC/N)	Sintering
1/9	93.1 ±0.7	16.2 ±1.2	1.0092	Tetragonal	97 ±2	1475 °C slow cooling
	87.6 ±0.5	20.9 ±2.3			104 ±3	1450 °C
	90.2 ±0.7	26.1 ±1.2			112 ±1	1475 °C
	90.0 ±2.5	26.1 ±1.4			113 ±1	1500 °C
3/7	94.6 ±1.3	17.2 ±1.9	1.0074	Tetragonal	184 ±2	1475 °C slow cooling
	92.8 ±1.1	17.6 ±1.0			175 ±4	1475 °C
	88.3 ±1.6	22.6 ±0.9			181 ±1	1450 °C
	92.5 ±1.5	28.9 ±1.4			192 ±2	1500 °C
4/6	91.7 ±1.4	13.6 ±1.6	1.0064	Tetragonal	250 ±9	1475 °C
	96.0 ±1.8	21.8 ±1.7			255 ±8	1425 °C
	89.2 ±0.2	33.4 ±2.7			268 ±9	1500 °C
	92.5 ±0.3	36.6 ±4.8			299 ±6	1525 °C
5/5	92.1 ±1.5	19.4 ±1.9	1.0043	Tetragonal +	301 ±34	1450 °C

	94.3 ±0.6	21.9 ±1.4		Orthorhombic	454 ±24	1475 °C
	96.3 ±0.6	31.5 ±1.0			466 ±21	1475 °C slow cooling
	95.6 ±1.5	33.1 ±1.2			387 ±27	1500 °C
6/4	94.8 ±1.9	17.0 ±2.2	-	Rhombohedral	213 ±17	1425 °C
	92.0 ±1.9	19.7 ±2.3			261 ±6	1450 °C
	88.8 ±0.7	28.4 ±3.1			295 ±10	1475 °C
	91.2 ±0.5	37.8 ±4.7			289 ±7	1500 °C
7/3	95.1 ±0.7	79.5 ±10.0	-	Rhombohedral	167 ±9	1525 °C
	97.6 ±0.5	79.8 ±8.3			165 ±14	1500 °C
	96.1 ±0.4	84.8 ±8.4			187 ±10	1425 °C
	98.1 ±0.6	84.9 ±10.7			190 ±21	1475 °C